

The portion of this research carried out at Northwestern University was supported by the NSF Synthetic Inorganic Organometallic Program (Grant No. CHE 8506011).

Supplementary Material Available: For the crystal structure of 3c,

listings of all thermal parameters, additional positional parameters, additional bond distances and angles, selected torsion angles, and selected intermolecular distances and a summary of crystal structure data (17 pages); a complete listing of observed and calculated structure factors (31 pages). Ordering information is given on any current masthead page.

Contribution from the Department of Chemistry,
University of South Carolina, Columbia, South Carolina 29208

Cluster Synthesis. 24. Synthesis and Characterization of New Sulfur-Containing Tungsten–Iron Carbonyl Cluster Complexes

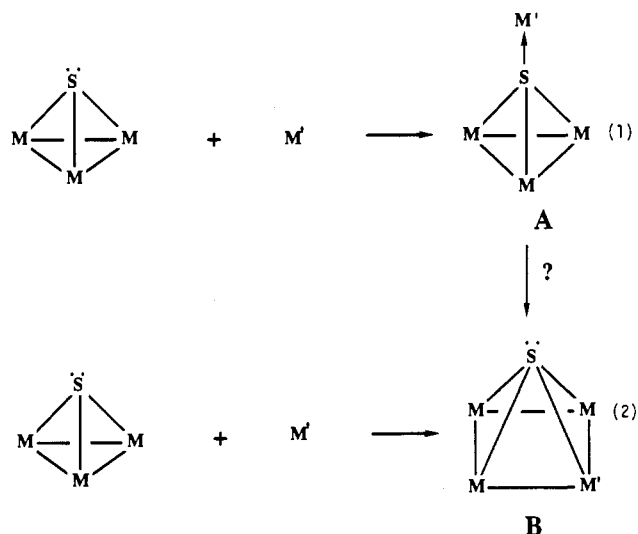
Richard D. Adams,* James E. Babin, Jin-Guu Wang, and Wengan Wu¹

Received September 29, 1988

The reaction of $\text{Fe}_3(\text{CO})_9(\mu_3\text{-S})_2$ (1) with $\text{W}(\text{CO})_6$ under UV irradiation yielded the $\text{W}(\text{CO})_5$ adduct, $\text{Fe}_3(\text{CO})_9(\mu_3\text{-S})(\mu_4\text{-S})[\text{W}(\text{CO})_5]$ (3), formed by the addition of the $\text{W}(\text{CO})_5$ group to one of the sulfido ligands in 1. The reaction of 1 with $\text{W}(\text{CO})_5(\text{PMe}_2\text{Ph})$ under UV irradiation yielded the related PMe_2Ph derivative of 3, $\text{Fe}_3(\text{CO})_9(\mu_3\text{-S})(\mu_4\text{-S})[\text{W}(\text{CO})_5(\text{PMe}_2\text{Ph})]$ (5), but also two new products $\text{WFe}_2(\text{CO})_9(\text{PMe}_2\text{Ph})(\mu_3\text{-S})_2$ (6) and $\text{WFe}_3(\text{CO})_{11}(\text{PMe}_2\text{Ph})(\mu_3\text{-S})_2$ (7). Compound 7 can be obtained by UV irradiation of 5. Compound 6 can be obtained from 7 in low yield by reaction with CO but was obtained in a better yield (40%) from the reaction of $\text{Fe}_2(\text{CO})_6(\mu\text{-S}_2)$ (2) with $\text{W}(\text{CO})_5(\text{PMe}_2\text{Ph})$ in the presence of UV irradiation. This reaction also yielded a $\text{W}(\text{CO})_5$ adduct of 6, $\text{WFe}_2(\text{CO})_9(\text{PMe}_2\text{Ph})(\mu_3\text{-S})(\mu_4\text{-S})[\text{W}(\text{CO})_5]$ (8), in very low yield, 3%. Compound 8 was obtained in 37% yield from the reaction of 6 with $\text{W}(\text{CO})_6$ under UV irradiation. Compounds 5–8 were characterized by X-ray crystallographic methods. For 5: space group $Pnma$, $a = 24.033$ (6) Å, $b = 14.226$ (4) Å, $c = 8.715$ (4) Å, $Z = 4$; solved by direct methods with $R = 0.028$ for 1579 reflections. For 6: space group $P2_1/n$, $a = 9.129$ (1) Å, $b = 15.878$ (6) Å, $c = 16.208$ (3) Å, $\beta = 91.52$ (1)°, $Z = 4$; solved by direct methods with $R = 0.029$ for 2477 reflections. For 7: space group $P1$, $a = 10.751$ (2) Å, $b = 13.776$ (3) Å, $c = 9.424$ (3) Å, $\alpha = 101.55$ (2)°, $\beta = 98.67$ (2)°, $\gamma = 76.34$ (1)°, $Z = 2$; solved by direct methods with $R = 0.024$ for 4069 reflections. For 8: space group $C2/c$, $a = 29.91$ (1) Å, $b = 13.427$ (3) Å, $c = 17.640$ (5) Å, $\beta = 120.48$ (2)°, $Z = 8$; solved by direct methods with $R = 0.027$ for 3418 reflections. The structure of 6 consists of an open WFe_2 cluster with two W–Fe bonds and triply bridging sulfido ligands on opposite sides of the cluster. The structure of 7 consists of a butterfly WFe_3 cluster with the tungsten atom in a hinge position. Sulfido ligands bridge the two closed Fe_2W triangular groups on opposite sides of the cluster. Compounds 5 and 8 are $\text{W}(\text{CO})_5\text{L}$ adducts of 1, $\text{L} = \text{PMe}_2\text{Ph}$, and 6, $\text{L} = \text{CO}$, respectively. The transformation of 5 to 7 is evidence that the sulfido ligand plays a key role in the metal-addition and cluster-forming processes. It is also believed that the lower electron density withdrawal capacity of the PMe_2Ph ligand compared to that of CO is one feature that promotes the stabilization of the W–Fe bonds observed in 6 and 7.

Introduction

Bridging ligands derived from the elements of the main groups have been found to play an important role, both in the synthesis and in the stabilization of transition-metal cluster complexes.^{2–7} Much of our recent research has been focused on systematics of the synthesis, structure, and bonding of sulfur-containing carbonyl clusters of ruthenium^{8–10} and osmium.⁷ We have shown that the sulfido ligand can promote the agglomeration of metal atoms by readily expanding its coordination number. Two examples of this are shown by eq 1¹¹ and 2.^{8–10} By the first route, sulfur uses its lone pair of electrons to donate to an empty orbital on a metal-containing group M' (A). In this reaction, no metal–metal bonds are formed. The sulfido ligand has a pseudotetrahedral geometry and serves as a neutral six-electron donor. By the second route, the metal-containing group is inserted into a metal–metal bond of the sulfido cluster B. Two metal–metal bonds and one



metal–sulfur bond are formed, and the square-pyramidal sulfido ligand serves as a four-electron donor. Species such as A could be key intermediates in the formation of B, but this has not yet been established.

We have previously investigated the reactions of $\text{Os}_3(\text{CO})_9(\mu_3\text{-S})_2$ with $\text{W}(\text{CO})_6$ and $\text{W}(\text{CO})_5(\text{PMe}_2\text{Ph})$.^{11,12} In this report is described our investigation of the reactions of $\text{Fe}_3(\text{CO})_9(\mu_3\text{-S})_2$

- (1) Visiting Scholar on leave from Zhenjiang Teacher's College, Zhenjiang, Jiangsu, People's Republic of China.
- (2) Whitmire, K. H. *J. Coord. Chem.* **1988**, 17, 95.
- (3) (a) Huttner, G.; Knoll, K. *Angew. Chem., Int. Ed. Engl.* **1987**, 26, 743. (b) Huttner, G.; Evertz, K. *Acc. Chem. Res.* **1986**, 19, 406.
- (4) Roberts, D. A.; Geoffroy, G. L. In *Comprehensive Organometallic Chemistry*; Wilkinson, G., Stone, F. G. A., Abel, E., Eds.; Pergamon: Oxford, England, 1982; Chapter 40.
- (5) Vahrenkamp, H. *Angew. Chem., Int. Ed. Engl.* **1975**, 322.
- (6) Gourdin, A.; Jeannin, Y. *J. Organomet. Chem.* **1986**, 304, C1.
- (7) Adams, R. D. *Polyhedron* **1985**, 4, 2003.
- (8) (a) Adams, R. D.; Babin, J. E.; Tasi, M. *Inorg. Chem.* **1986**, 25, 4514. (b) Adams, R. D.; Babin, J. E.; Tasi, M. *Inorg. Chem.* **1987**, 26, 2807.
- (9) Adams, R. D.; Babin, J. E.; Tasi, M. *Organometallics* **1988**, 7, 503.
- (10) Adams, R. D.; Babin, J. E.; Tasi, M. *Inorg. Chem.* **1986**, 25, 4460.
- (11) Adams, R. D.; Horvath, I. T.; Wang, S. *Inorg. Chem.* **1985**, 22, 1728.

- (12) Adams, R. D.; Horvath, I. T.; Mathur, P. *J. Am. Chem. Soc.* **1984**, 106, 6292.

Table I. Crystallographic Data for the Structural Analyses of Compounds 5–8

	5	6	7	8
	Crystal Data			
formula	WFe ₃ S ₂ PO ₁₃ C ₂₁ H ₁₁	WFe ₂ S ₂ PO ₉ C ₁₇ H ₁₁	WFe ₃ S ₂ PO ₁₁ C ₁₉ H ₁₁	W ₂ Fe ₂ S ₂ PO ₁₄ C ₂₂ H ₁₁
temp (±3), °C	23	23	23	23
space group	<i>Pnma</i> , No. 62	<i>P2₁/n</i> , No. 14	<i>P1</i> , No. 2	<i>C2/c</i> , No. 15
<i>a</i> , Å	24.033 (6)	9.129 (1)	10.751 (2)	29.91 (1)
<i>b</i> , Å	14.226 (4)	15.878 (6)	13.776 (3)	13.427 (3)
<i>c</i> , Å	8.715 (4)	16.208 (3)	9.424 (3)	17.640 (5)
α , deg	90.0	90.0	101.55 (2)	90.0
β , deg	90.0	91.52 (1)	98.67 (2)	120.48 (2)
γ , deg	90.0	90.0	76.34 (1)	90.0
<i>V</i> , Å ³	2979 (2)	2348 (1)	1321.0 (6)	6105 (3)
<i>M_r</i>	917.79	749.9	861.8	1073.81
<i>Z</i>	4	4	2	8
ρ_{calc} , g/cm ³	2.05	2.12	2.17	2.34
	Treatment of Data			
abs cor: type; coeff, cm ⁻¹	analytical; 57.9	empirical; 67.0	empirical; 65.1	analytical; 91.5
transmission coeff: max; min	0.93; 0.29	1.00; 0.68	1.00; 0.51	0.56; 0.21
final resid: <i>R_F</i> ; <i>R_{wF}</i>	0.028; 0.028	0.029; 0.031	0.024; 0.027	0.027; 0.027

(1) and Fe₂(CO)₆(μ-S₂) (2) with W(CO)₆ and W(CO)₅(PMe₂Ph). These results are compared with those of the osmium system.

Experimental Section

Although the reagents and starting materials are air stable, all reactions were performed under a dry nitrogen atmosphere. Reagent grade solvents were dried over molecular sieves and were deoxygenated with N₂ prior to use. PMe₂Ph was purchased from Aldrich and was used without further purification. Photolysis experiments were performed by using an external high-pressure mercury lamp on reaction solutions contained in Pyrex glassware. IR spectra were recorded on a Nicolet 5-DXB FT-IR spectrophotometer. ¹H NMR spectra were run on a Bruker AM-300 spectrometer operating at 300 MHz. TLC separations were performed on plates (0.25-mm Kieselgel 60 F₂₅₄, E. Merck). W(CO)₆ was purchased from Strem Chemicals, Newburyport, MA. W(CO)₅(PMe₂Ph)¹³ and Fe₂(CO)₆(μ-S₂) (2)¹⁴ were prepared by reported procedures. Fe₃(CO)₉(μ₃-S)₂ (1) was made by the method of King by using (CH₂)₂S instead of C₆H₁₀S.¹⁵

Reaction of 1 with W(CO)₆ in the Presence of UV Irradiation. A solution of 1 (50 mg, 0.10 mmol) and W(CO)₆ (170 mg, 0.48 mmol) in 50 mL of hexane was photolyzed under a continuous purge of nitrogen for 4 h. A black precipitate formed. The solution (almost colorless) was decanted, and the precipitate was washed with hexane (2 mL per portion) three times. The precipitate was then dissolved in a minimum of CH₂Cl₂, and the solution was chromatographed by TLC, eluting with CH₂Cl₂/hexane, (1/9) to yield 18.3 mg of dark brown Fe₃(CO)₉(μ₃-S)(μ₄-S)[W(CO)₅] (3), 23% yield.

Reaction of 1 with W(CO)₅(PMe₂Ph) in the Presence of UV Irradiation. (a) **2-h Irradiation.** A mixture of 1 (75 mg, 0.155 mmol) and W(CO)₅(PMe₂Ph) (135 mg, 0.292 mmol) was dissolved in 130 mL of hexane solvent, and the solution was photolyzed under a continuous purge with N₂ for 2 h. The color of the solution changed from red to brown. The solvent was removed in vacuo, and the brown residue was dissolved in 1 mL of CH₂Cl₂ and the mixture separated by TLC.

Elution with a hexane/CH₂Cl₂ (8/2) mixture separated (in order of elution) Fe₂(CO)₆(μ-S₂) (2) (1.4 mg, 2.6%), unreacted 1 (21.0 mg), black Fe₃(CO)₉(μ₃-S)(μ₄-S)[W(CO)₅] (3) (3.1 mg, 2.5%), unreacted W(CO)₅(PMe₂Ph) (8.7 mg), Fe₃(CO)₉(PMe₂Ph)(μ₃-S)₂¹⁶ (4) (2.3 mg, 2.5%), a trace of violet Fe₃(CO)₉(μ₃-S)(μ₄-S)[W(CO)₄(PMe₂Ph)] (5), red-brown WFe₂(CO)₉(PMe₂Ph)(μ₃-S)₂ (6) (1.5 mg, 1.3%), and dark brown WFe₃(CO)₁₁(PMe₂Ph)(μ₃-S)₂ (7) (30.7 mg, 23%).

(b) **40-min Irradiation.** A mixture of 1 (45 mg, 0.092 mmol) and W(CO)₅(PMe₂Ph) (40 mg, 0.0866 mmol) was dissolved in 60 mL of hexane, and the solution was photolyzed for 40 min while being stirred and continuously purged with nitrogen. Workup as described above (part a) yielded 24 mg of 1 followed by 3.7 mg of 5 (9.2% based on the amount of 1 consumed) and only a trace (1.2 mg) of 7.

Photolysis of 5. Compound 5 (20 mg, 0.0218 mmol) was dissolved in 25 mL of hexane, and the solution was photolyzed under a continuous purge of nitrogen for 25 min. The solvent was removed in vacuo, and the residue was separated by TLC using hexane solvent. The following

bands were obtained in order of elution: trace amounts of W(CO)₆ and Fe₂S₂(CO)₆; 1.9 mg of 1 (18%); 1.0 mg of W(CO)₅(PMe₂Ph) (9.9%); 1.5 mg of 4 (12%); 1.4 mg of unreacted 5; 1.2 mg of 6 (7%); 4.2 mg of 7 (22%).

Preparation of 6. Compound 2 (30 mg, 0.087 mmol) and W(CO)₅(PMe₂Ph) (100 mg, 0.216 mmol) were dissolved in 30 mL of hexane solvent, and then the solution was irradiated in the presence of a nitrogen purge for 2.5 h. The solution turned to red-brown, and a small amount of black precipitate formed. The solvent was removed in vacuo. The brown residue was transferred to silica gel TLC plates and was eluted with hexane. Six bands were eluted. These were identified as 2 (0.5 mg, 1.7%), 1 (0.9 mg, 2.1%), unreacted W(CO)₅(PMe₂Ph) (34.4 mg), 6 (26.0 mg, 40%), and violet WFe₂(CO)₉(PMe₂Ph)(μ₃-S)(μ₄-S)[W(CO)₅] (8) (2.9 mg, 3%).

Reaction of 6 with W(CO)₆. Compound 6 (13 mg, 0.017 mmol) and W(CO)₆ (30 mg, 0.085 mmol) were dissolved in 15 mL of hexane, and then the solution was irradiated under a continuous purge of nitrogen for 30 min. The solution changed from red-brown to dark brown. The solvent was removed in vacuo, and the brown residue was separated by TLC on silica gel. Elution with hexane/CH₂Cl₂ (9/1) yielded 6.7 mg of 8 (37%).

Reaction of 7 with CO. Compound 7 (30 mg, 0.035 mmol) was dissolved in 50 mL of hexane. The solution was heated to reflux under a continuous purge of CO for 2 h. The solvent was removed in vacuo, and the brown residue was separated by TLC with hexane solvent. In order of elution the following compounds were obtained: 2 (0.2 mg, 2%); 1 (10.2 mg, 60%); W(CO)₅(PMe₂Ph) (9.7 mg, 60%); 4 (1.7 mg, 8.2%); 6 (1.5 mg, 6%); 3.8 mg of unreacted 7.

Crystallographic Analyses. Opaque violet crystals of 5 were grown by slow evaporation of solvent from CH₂Cl₂/hexane 1/4 solutions at 10 °C. Opaque brown crystals of 6 were grown by slow evaporation of solvent from hexane/CH₂Cl₂ 4/1 solutions at -20 °C. Opaque brown crystals of 7 were grown by slow evaporation of solvent from CH₂Cl₂/hexane 1/4 solutions at 10 °C, and opaque violet crystals of 8 were grown similarly from CH₂Cl₂/hexane 3/7 solutions at 10 °C. All data crystals were mounted in thin-walled glass capillaries. Diffraction measurements were made on a Rigaku AFC6 automatic diffractometer using graphite-monochromatized Mo K α radiation. Unit cells were determined from 25 randomly selected reflections obtained by using the AFC6 automatic search, center, index, and least-squares routines. Crystal data and results of the analyses are listed in Table I. All data processing was performed on a Digital Equipment Corp. MICROVAX II computer by using the TEXSAN structure-solving program library (v 2.0) obtained from Molecular Structure Corp., College Station, TX. Neutral-atom scattering factors were calculated by the standard procedures.^{17a} Anomalous dispersion corrections were applied to all non-hydrogen atoms.^{17b} Full-matrix least-squares refinements minimized the function $\sum_{hkl} w - (|F_o| - |F_c|)^2$, where $w = 1/\sigma(F)^2$, $\sigma(F) = \sigma(F_o^2)/2F_o$, and $\sigma(F_c^2) = [\sigma(I_{\text{raw}})^2 + (PF_o^2)^2]^{1/2}/Lp$. All the structures were solved by direct methods by using the program MITHRIL. The positions of the hydrogen atoms on the phosphine ligand were calculated by assuming idealized geometries for the phenyl and methyl groups and using located positions whenever possible. Their scattering contributions were added to the structure factor

(13) Mathieu, R.; Lenzi, M.; Poilblanc, R. *Inorg. Chem.* **1970**, *9*, 2030.

(14) Nametkin, N. S.; Tyurin, V. D.; Kukima, J. *Organomet. Chem.* **1978**, *149*, 355.

(15) King, R. B. *Inorg. Chem.* **1963**, *2*, 326.

(16) Cetini, O.; Stanghellini, P. L. K.; Rossetti, R.; Gambino, O. *J. Organomet. Chem.* **1968**, *15*, 373.

(17) *International Tables for X-ray Crystallography*; Kynoch Press: Birmingham, England, 1975; Vol. IV: (a) Table 2.2B, pp 99–101; (b) Table 2.3.1, pp 149–150.

Table II. Spectroscopic and Analytical Data for the Compounds Prepared in This Study

compd	IR: $\nu(\text{CO})$, cm^{-1} (in hexane)	$^1\text{H NMR}$: δ (in CDCl_3)	anal., % found (calc)	
			C	H
3	2069 (vs), 2066 (sh), 2051 (vs), 2029 (m), 2019 (sh), 1953 (vs)		21.48 (20.82)	
5	2090 (vw), 2060 (s), 2042 (vs), 2027 (s), 2016 (w), 2008 (w), 2002 (sh), 1939 (w), 1913 (sh), 1910 (m)	7.42 (m, 5 H), 1.93 (d, 6 H, $J_{\text{PH}} = 8.0$ Hz)	27.26 (27.48)	1.30 (1.21)
6	2074 (m), 2041 (vs), 2019 (vs), 1999 (m), 1993 (m), 1990 (m), 1971 (m), 1933 (w, br)	7.54-7.79 (m, 5 H), 2.23 (d, 6 H, $J_{\text{PH}} = 9.0$ Hz)	27.32 (27.23)	1.37 (1.45)
7	2074 (w), 2042 (vs), 2020 (m), 2001 (s), 1993 (m), 1981 (m), 1972 (w), 1952 (w), 1874 (w, br)	7.48 (m, 5 H), 2.04 (d, 6 H, $J_{\text{PH}} = 9.0$ Hz)	26.36 (26.48)	1.13 (1.29)
8	2087 (m), 2063 (s), 2050 (vs), 2027 (vs), 2009 (m), 2004 (m), 1995 (sh), 1983 (w), 1968 (vw), 1954 (m), 1944 (s), 1934 (s), 1908 (w)	7.66 (m, 5 H), 2.32 (d, 3 H, $J_{\text{PH}} = 9.8$ Hz), 2.26 (d, 3 H, $J_{\text{PH}} = 9.5$ Hz)	24.53 (24.61)	0.90 (1.03)

calculations, but their positions were not refined.

The systematic absences observed in the data for compound **5** were consistent with either of the space groups $Pnma$ or $Pna2_1$. The higher symmetry group $Pnma$ was chosen and confirmed by the successful solution and refinement of the structure. The space group $P2_1/n$ was identified uniquely by the systematic absences observed in the data for **6**. Compound **7** crystallized in the triclinic crystal system. The centrosymmetric space group $P\bar{1}$ was assumed and confirmed by the successful solution and refinement of the structure. The systematic absences in the data for **8** were consistent with either of the space groups Cc or $C2/c$. The higher symmetry group $C2/c$ was chosen and confirmed by the successful solution and refinement of the structure.

Results

When solutions of **1** and $\text{W}(\text{CO})_6$ were subjected to UV irradiation, decarbonylation of $\text{W}(\text{CO})_6$ occurred and the product $\text{Fe}_3(\text{CO})_9(\mu_3\text{-S})(\mu_4\text{-S})[\text{W}(\text{CO})_5]$ (**3**) was formed by the addition of a $\text{W}(\text{CO})_5$ fragment to one of the triply bridging sulfido ligands of **1**. On the basis of their very similar IR spectra (see Table II), compound **3** is believed to be structurally similar to its osmium homologue, which has been characterized crystallographically,¹¹ and to its phosphine-substituted derivative $\text{Fe}_3(\text{CO})_9(\mu_3\text{-S})(\mu_4\text{-S})[\text{W}(\text{CO})_4(\text{PMe}_2\text{Ph})]$ (**5**), which is described below.

When solutions of **1** and $\text{W}(\text{CO})_5(\text{PMe}_2\text{Ph})$ were exposed to UV irradiation for short periods of time, the principal product was **5**, although the yield was low (~10%). Small amounts of a second product $\text{WFe}_3(\text{CO})_{11}(\text{PMe}_2\text{Ph})(\mu_3\text{-S})_2$ (**7**) were also formed. For reactions with longer irradiation exposure periods, the yield of **7** was increased greatly (23%), and only traces of **5** were obtained. In addition, several minor products $\text{Fe}_2(\text{CO})_8(\mu\text{-S}_2)$ (**2**) (2.6%), $\text{Fe}_3(\text{CO})_8(\text{PMe}_2\text{Ph})(\mu_3\text{-S})_2$,¹⁶ (**4**) (2.5%), and $\text{WFe}_2(\text{CO})_9(\text{PMe}_2\text{Ph})(\mu_3\text{-S})_2$ (**6**) (1.3%) were formed. Compounds **3** and **5-7** are new, and their IR and $^1\text{H NMR}$ spectra are reported in Table II. These results suggested that **5** was converted to **7** photolytically, and this was confirmed independently by the irradiation of a sample of **5**, which produced **7** in 22% yield. The transformation of **5** to **7** could not be achieved by thermal activation.

Since compound **6** contains one less iron atom than **7**, an attempt was made to prepare **6** from **7** by cleavage of an iron grouping by using carbon monoxide. However, although small amounts of **6** were obtained, the principal products were **1** and $\text{W}(\text{CO})_5(\text{PMe}_2\text{Ph})$, formed by cleavage of the tungsten grouping. Seyferth has reported the formation of $\text{Fe}_2\text{Pt}(\text{CO})_6(\text{PPh}_3)_2(\mu_3\text{-S})_2$ from the reaction of **2** with $\text{Pt}(\text{PPh}_3)_2$.¹⁸ Accordingly, the reaction of **2** with $\text{W}(\text{CO})_5(\text{PMe}_2\text{Ph})$ under UV irradiation was attempted and found to give **6** in a much better yield (40%). This preparation of **6** also yielded small amounts of the compound $\text{WFe}_2(\text{CO})_9(\text{PMe}_2\text{Ph})(\mu_3\text{-S})(\mu_4\text{-S})[\text{W}(\text{CO})_5]$ (**8**). As shown below, **8** is simply a $\text{W}(\text{CO})_5$ adduct of **6** and it was found that **8** could be made in a much better yield (37%) by the irradiation of a mixture of **6** and $\text{W}(\text{CO})_6$. IR and $^1\text{H NMR}$ spectra of **8** are listed in Table II. Compounds **5-8** were also characterized by single-crystal X-ray diffraction analyses.

Description of the Structures. Structure of 5. An ORTEP drawing of the molecular structure of **5** is shown in Figure 1. Intramolecular bond distances and selected bond angles are listed

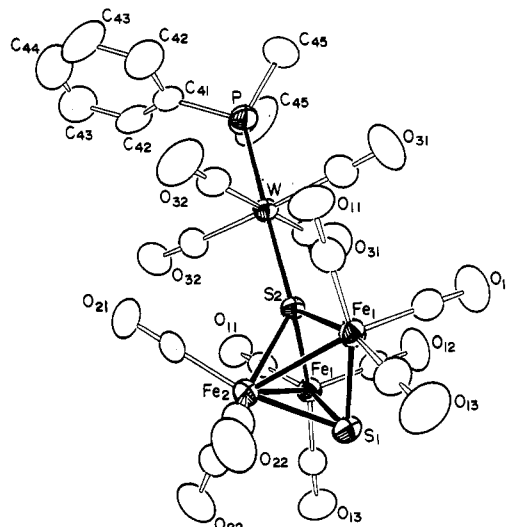


Figure 1. ORTEP drawing of $\text{Fe}_3(\text{CO})_9(\mu_3\text{-S})(\mu_4\text{-S})[\text{W}(\text{CO})_4\text{PMe}_2\text{Ph}]$ (**5**).

Table III. Intramolecular Distances (Å) for **5**

W-C31	2.008 (9)	Fe1-Fe2	2.606 (2)
W-C32	2.020 (9)	Fe2-C22	1.781 (9)
W-S2	2.433 (3)	Fe2-C21	1.81 (1)
W-P	2.443 (3)	Fe2-S1	2.250 (3)
Fe1-C12	1.782 (8)	Fe2-S2	2.255 (3)
Fe1-C13	1.804 (8)	P-C45	1.81 (1)
Fe1-C11	1.820 (8)	P-C41	1.82 (1)
Fe1-S2	2.224 (2)	O-C(av)	1.135 (8)
Fe1-S1	2.233 (2)	C-C(av)	1.36 (1)

Table IV. Intramolecular Bond Angles (deg) for **5**

C31-W-S2	89.7 (3)	C22-Fe2-Fe1	147.3 (3)
C31-W-P	89.3 (3)	C21-Fe2-S1	167.3 (3)
C32-W-S2	92.7 (2)	C21-Fe2-S2	88.3 (3)
C32-W-P	88.3 (2)	C21-Fe2-Fe1	117.7 (2)
S2-W-P	178.7 (1)	S1-Fe2-S2	79.0 (1)
C12-Fe1-S2	96.7 (3)	S1-Fe2-Fe1	54.14 (6)
C12-Fe1-S1	99.0 (3)	S2-Fe2-Fe1	53.85 (5)
C12-Fe1-Fe2	141.5 (2)	Fe1-Fe2-Fe1'	80.77 (6)
C13-Fe1-S2	165.2 (3)	Fe1-S1-Fe1'	98.3 (1)
C13-Fe1-S1	90.4 (2)	Fe1-S1-Fe2	71.10 (8)
C13-Fe1-Fe2	110.3 (3)	Fe1-S2-Fe1'	98.8 (1)
C11-Fe1-S2	93.6 (2)	Fe1-S2-Fe2	71.17 (7)
C11-Fe1-S1	161.7 (3)	Fe1-S2-W	128.04 (6)
C11-Fe1-Fe2	107.6 (2)	Fe2-S2-W	138.4 (1)
S2-Fe1-S1	80.01 (8)	C45-P-W	116.9 (4)
S2-Fe1-Fe2	54.97 (8)	C41-P-W	113.3 (4)
S1-Fe1-Fe2	54.76 (8)	C42-C41-C42	118 (1)
C22-Fe2-S1	93.3 (3)	C42-C41-P	120.9 (6)
C22-Fe2-S2	130.1 (3)	O-C(av)-Fe	177 (1)
C22-Fe2-Fe1	81.6 (3)	O-C(av)-W	178 (1)

in Tables III and IV. The molecule contains a crystallographically imposed plane of symmetry that passes through the atoms S1, Fe2, S2, W, P, C41, C44, C21, and O21. The molecule can be viewed as a combination of molecule **1** and a $\text{W}(\text{CO})_4(\text{PMe}_2\text{Ph})$ fragment joined by a donor-acceptor bond between the sulfur atom

(18) Seyferth, D.; Henderson, R. S.; Gallagher, M. K. *J. Organomet. Chem.* **1980**, *193*, C75.

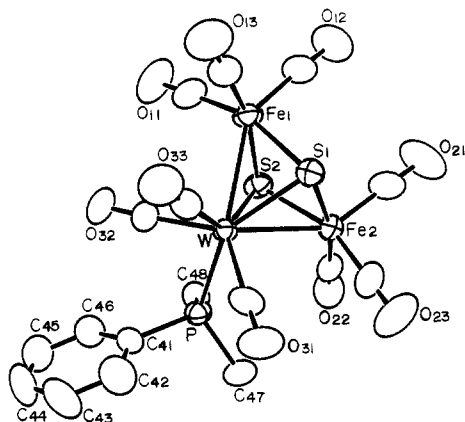
Figure 2. ORTEP drawing of $WFe_2(CO)_9(PMe_2Ph)(\mu_3-S)_2$ (6).

Table V. Intramolecular Distances (Å) for 6

W-C33	2.00 (1)	Fe1-S2	2.252 (3)
W-C32	2.00 (1)	Fe2-C23	1.76 (1)
W-C31	2.02 (1)	Fe2-C22	1.78 (1)
W-S1	2.420 (2)	Fe2-C21	1.79 (1)
W-S2	2.429 (2)	Fe2-S2	2.246 (3)
W-P	2.521 (2)	Fe2-S1	2.261 (3)
W-Fe1	2.762 (1)	P-C48	1.802 (9)
W-Fe2	2.770 (1)	P-C47	1.812 (9)
Fe1-C11	1.79 (1)	P-C41	1.813 (9)
Fe1-C13	1.79 (1)	O-C(av)	1.140 (1)
Fe1-C12	1.80 (1)	C-C(av)	1.370 (2)
Fe1-S1	2.250 (3)		

Table VI. Intramolecular Bond Angles (deg) for 6

C33-W-S1	85.7 (3)	C13-Fe1-S2	162.0 (3)
C33-W-S2	135.4 (3)	C13-Fe1-W	105.8 (3)
C33-W-P	125.6 (3)	C12-Fe1-S1	97.2 (3)
C33-W-Fe1	85.5 (2)	C12-Fe1-S2	97.9 (3)
C33-W-Fe2	135.5 (3)	C12-Fe1-W	143.8 (3)
C32-W-S1	137.3 (3)	S1-Fe1-S2	80.93 (9)
C32-W-S2	92.8 (3)	S1-Fe1-W	56.62 (6)
C32-W-P	75.6 (3)	S2-Fe1-W	56.87 (6)
C32-W-Fe1	89.0 (3)	C23-Fe2-S2	156.2 (4)
C32-W-Fe2	142.1 (3)	C23-Fe2-S1	93.0 (3)
C31-W-S1	92.6 (3)	C23-Fe2-W	100.7 (3)
C31-W-S2	139.9 (3)	C22-Fe2-S2	89.5 (3)
C31-W-P	77.0 (2)	C22-Fe2-S1	167.5 (3)
C31-W-Fe1	141.5 (2)	C22-Fe2-W	111.6 (3)
C31-W-Fe2	91.4 (3)	C21-Fe2-S2	103.8 (4)
S1-W-S2	74.11 (8)	C21-Fe2-S1	94.2 (3)
S1-W-P	142.96 (7)	C21-Fe2-W	144.8 (3)
S1-W-Fe1	50.95 (6)	S2-Fe2-S1	80.84 (9)
S1-W-Fe2	51.11 (6)	S2-Fe2-W	56.79 (6)
S2-W-P	91.04 (8)	S1-Fe2-W	56.41 (6)
S2-W-Fe1	50.92 (6)	Fe1-S1-Fe2	97.5 (1)
S2-W-Fe2	50.67 (6)	Fe1-S1-W	72.42 (7)
P-W-Fe1	138.63 (6)	Fe2-S1-W	72.48 (7)
P-W-Fe2	93.15 (6)	Fe2-S2-Fe1	97.9 (1)
Fe1-W-Fe2	75.62 (4)	Fe2-S2-W	72.54 (7)
C11-Fe1-S1	162.3 (3)	Fe1-S2-W	72.20 (7)
C11-Fe1-S2	89.8 (3)	O-C-Fe(av)	178 (4)
C11-Fe1-W	105.7 (3)	O-C-W(av)	177 (1)
C13-Fe1-S1	93.3 (3)		

S2 and the tungsten atom. Compound **5** is structurally similar to $Os_3(CO)_9(\mu_3-S)(\mu_4-S)[W(CO)_5]$ (**9**) and $Fe_3(CO)_9(\mu_3-P-t-Bu)(\mu_4-S)[W(CO)_5]$ (**10**).¹⁹ The $Fe_3(CO)_9(\mu_3-S)_2$ portion of **5** is not significantly different structurally from the free molecule **1**.²⁰ The W-S distance, 2.433 (3) Å, is significantly shorter than that in **9**, 2.522 (8) Å, and **10**, 2.547 (6) Å. This may be due to the weaker trans-directing influence of the PMe_2Ph ligand in **5** compared to that of the trans CO ligand in **9** and **10**.

Structure of 6. An ORTEP drawing of the molecular structure of **6** is shown in Figure 2. Intramolecular bond distances and

Table VII. Intramolecular Distances (Å) for 7

W-C41	2.038 (5)	Fe2-C22	1.764 (6)
W-C43	2.054 (6)	Fe2-C21	1.785 (7)
W-C42	2.078 (5)	Fe2-S1	2.194 (2)
W-S2	2.375 (1)	Fe2-S2	2.209 (2)
W-S1	2.383 (1)	Fe2-Fe3	2.567 (1)
W-P	2.546 (2)	Fe3-C31	1.783 (6)
W-Fe2	2.677 (1)	Fe3-C32	1.797 (6)
W-Fe3	2.8067 (9)	Fe3-C33	1.798 (7)
W-Fe1	2.832 (1)	Fe3-S1	2.184 (2)
Fe1-C11	1.787 (6)	P-C58	1.792 (7)
Fe1-C12	1.788 (6)	P-C57	1.797 (6)
Fe1-C13	1.796 (6)	P-C51	1.804 (5)
Fe1-S2	2.183 (2)	O-C(av)	1.133 (7)
Fe1-Fe2	2.557 (1)	C-C(av)	1.37 (1)

Table VIII. Intramolecular Bond Angles (deg) for 7

C41-W-S2	87.7 (1)	C22-Fe2-S1	133.2 (2)
C41-W-S1	108.2 (2)	C22-Fe2-S2	95.1 (2)
C41-W-P	80.1 (2)	C22-Fe2-Fe1	131.7 (2)
C41-W-Fe2	99.9 (1)	C22-Fe2-Fe3	87.1 (2)
C41-W-Fe3	60.5 (2)	C22-Fe2-W	132.6 (2)
C41-W-Fe1	136.3 (1)	C21-Fe2-S1	94.5 (2)
C43-W-S2	105.4 (2)	C21-Fe2-S2	132.0 (2)
C43-W-S1	87.4 (2)	C21-Fe2-Fe1	87.9 (2)
C43-W-P	82.0 (2)	C21-Fe2-Fe3	127.6 (2)
C43-W-Fe2	102.8 (2)	C21-Fe2-W	136.9 (2)
C43-W-Fe3	136.1 (2)	S1-Fe2-S2	114.61 (6)
C43-W-Fe1	59.7 (2)	S1-Fe2-Fe1	95.03 (5)
C42-W-S2	170.3 (2)	S1-Fe2-Fe3	53.93 (4)
C42-W-S1	83.4 (2)	S1-Fe2-W	57.55 (4)
C42-W-P	87.9 (2)	S2-Fe2-Fe1	53.92 (4)
C42-W-Fe2	133.1 (1)	S2-Fe2-Fe3	100.27 (5)
C42-W-Fe3	88.0 (2)	S2-Fe2-W	57.20 (4)
C42-W-Fe1	140.7 (2)	Fe1-Fe2-Fe3	129.97 (4)
S2-W-S1	102.32 (5)	Fe1-Fe2-W	65.46 (3)
S2-W-P	87.76 (5)	Fe3-Fe2-W	64.67 (3)
S2-W-Fe2	51.44 (4)	C31-Fe3-S1	91.2 (2)
S2-W-Fe3	89.91 (4)	C31-Fe3-Fe2	89.4 (2)
S2-W-Fe1	48.61 (4)	C31-Fe3-W	143.1 (2)
S1-W-P	166.99 (5)	C32-Fe3-S1	105.3 (2)
S1-W-Fe2	50.99 (4)	C32-Fe3-Fe2	158.8 (2)
S1-W-Fe3	48.95 (4)	C32-Fe3-W	105.8 (2)
S1-W-Fe1	84.20 (4)	C33-Fe3-S1	154.2 (2)
P-W-Fe2	138.98 (4)	C33-Fe3-Fe2	100.4 (2)
P-W-Fe3	140.51 (4)	C33-Fe3-W	110.5 (2)
P-W-Fe1	96.71 (4)	S1-Fe3-Fe2	54.27 (4)
Fe2-W-Fe3	55.77 (3)	S1-Fe3-W	55.35 (4)
Fe2-W-Fe1	55.22 (3)	Fe2-Fe3-W	59.56 (3)
Fe3-W-Fe1	110.88 (3)	Fe3-S1-Fe2	71.80 (5)
C11-Fe1-S2	90.8 (2)	Fe3-S1-W	75.70 (5)
C11-Fe1-Fe2	87.1 (2)	Fe1-S2-Fe2	71.46 (5)
C11-Fe1-W	141.0 (2)	Fe1-S2-W	71.19 (5)
C12-Fe1-S2	109.2 (2)	Fe2-S2-W	71.36 (4)
C12-Fe1-Fe2	164.1 (2)	C58-P-W	115.1 (2)
C12-Fe1-W	114.2 (2)	C57-P-W	118.8 (2)
C13-Fe1-S2	150.5 (2)	C51-P-W	110.4 (2)
C13-Fe1-Fe2	96.4 (2)	O41-C41-W	164.0 (5)
C13-Fe1-W	107.2 (2)	O42-C42-W	178.5 (5)
S2-Fe1-Fe2	54.88 (4)	O43-C43-W	163.3 (5)
S2-Fe1-W	54.70 (4)	O-C(av)-Fe	178.0 (8)
Fe2-Fe1-W	59.32 (3)		

selected bond angles are listed in Tables V and VI. The molecule consists of an open WFe_2 cluster that is bridged on opposite sides by triply bridging sulfido ligands. The cluster is structurally very similar to **1**,²⁰ but contains a $W(CO)_3(PMe_2Ph)$ grouping in the center instead of a $Fe(CO)_3$ group. The W-Fe bond distances are very similar to each other, 2.762 (1) and 2.770 (2) Å, and to the W-Fe bond distance of 2.792 (2) Å observed in the sulfur-bridged mixed-metal cluster complex $CoFeW(CO)_7(PMe_2Ph)(\mu_3-S)$.²¹ All the CO ligands are linear ($M-C-O = 177-180^\circ$). The PMe_2Ph ligand that is coordinated to the tungsten atom exhibits no unusual structural features. The compound

(19) Winter, A.; Jibril, I.; Huttner, G. *J. Organomet. Chem.* **1983**, *247*, 259.
 (20) Wei, C. H.; Dahl, L. F. *Inorg. Chem.* **1965**, *4*, 493.

(21) Richter, F.; Vahrenkamp, H. *J. Organomet. Chem.* **1980**, *190*, C67.

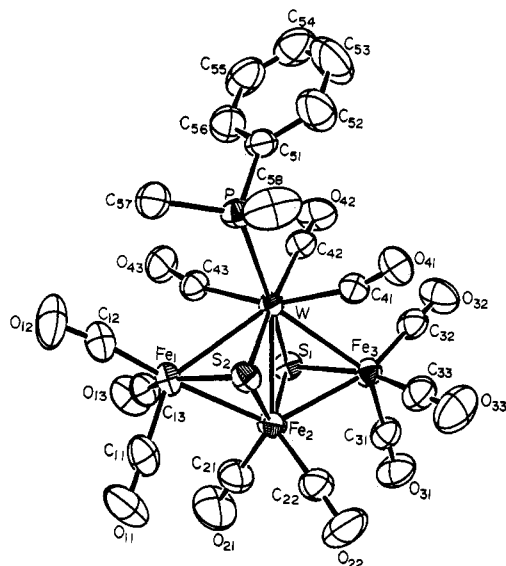


Figure 3. ORTEP drawing of $WFe_3(CO)_{11}(PMe_2Ph)(\mu_3-S)_2$ (7).

Table IX. Intramolecular Distances (Å) for 8

W1-C11	1.95 (1)	Fe1-C31	1.791 (9)
W1-C12	2.03 (1)	Fe1-C33	1.79 (1)
W1-C15	2.04 (1)	Fe1-S1	2.245 (2)
W1-C14	2.05 (1)	Fe1-S2	2.252 (3)
W1-C13	2.05 (1)	Fe2-C41	1.778 (9)
W1-S1	2.537 (2)	Fe2-C43	1.80 (1)
W2-C21	1.99 (1)	Fe2-C42	1.82 (1)
W2-C22	2.00 (1)	Fe2-S1	2.247 (3)
W2-C23	2.01 (1)	Fe2-S2	2.263 (2)
W2-S1	2.417 (2)	P-C57	1.80 (1)
W2-S2	2.434 (2)	P-C58	1.81 (1)
W2-P	2.523 (2)	P-C51	1.819 (9)
W2-Fe2	2.780 (2)	O-C(av)	1.13 (1)
W2-Fe1	2.794 (1)	C-C(av)	1.36 (1)
Fe1-C32	1.78 (1)		

$Fe_2Co(CO)_6(C_5H_4CO_2Me)(\mu_3-S)_2$ is also structurally similar to 6.²²

Structure of 7. An ORTEP drawing of the molecular structure of 7 is shown in Figure 3. Intramolecular bond distances and selected bond angles are listed in Tables VII and VIII. The molecule consists of a butterfly cluster containing one tungsten and three iron atoms with the tungsten atom occupying one of the "hinge" positions. The dihedral angle between the two WFe_2 planes is 167° . Triply bridging sulfido ligands bridge the two closed triangular faces and lie on opposite sides of the cluster. The two peripheral tungsten-iron bonds are similar in length, 2.806 (9) Å, and slightly longer than those in 6. The diagonal bond, W-Fe2, at 2.677 (1) Å is significantly shorter than all the others. The iron-iron bonds, 2.557 (1) and 2.567 (1) Å, are slightly shorter than those in 1 and 5. The tungsten-sulfur bonds, 2.375 (1) and 2.383 (1) Å, are significantly shorter (0.05 Å) than those in 6. The tungsten atom has an extraordinarily crowded coordination that includes nine nearest neighbors. There are 11 carbonyl ligands. Those on the iron atoms are linear, but two of the three on the tungsten atom exhibit a semibridging character toward the wing-tip iron atoms, W-C41-O41 = $164.0(5)^\circ$ and W-C43-O43 = $163.3(5)^\circ$. The PMe_2Ph ligand is coordinated to the tungsten atom and exhibits no unusual structural distortions. Overall, compound 7 contains 62 valence electrons and is thus electron precise; however, for each metal atom to have an 18-electron configuration one of the tungsten-iron bonds would have to be viewed as a tungsten to iron donor-acceptor bond. Semibridging carbonyl ligands frequently accompany the formation of donor-acceptor metal-metal bonds, and this is the case with 7 also.²³

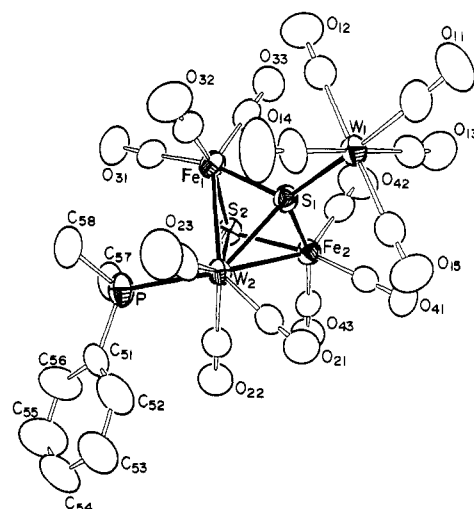


Figure 4. ORTEP drawing of $WFe_2(CO)_5(PMe_2Ph)(\mu_3-S)(\mu_4-S)[W(CO)_5]$ (8).

Table X. Intramolecular Bond Angles (deg) for 8

C11-W1-S1	172.4 (3)	C31-Fe1-S1	166.3 (3)
C12-W1-S1	88.1 (3)	C31-Fe1-S2	92.4 (3)
C15-W1-S1	96.0 (2)	C31-Fe1-W2	110.3 (3)
C14-W1-S1	94.0 (3)	C33-Fe1-S1	95.2 (3)
C13-W1-S1	86.9 (3)	C33-Fe1-S2	101.5 (3)
C21-W2-S1	86.8 (2)	C33-Fe1-W2	144.2 (3)
C21-W2-S2	135.8 (3)	S1-Fe1-S2	79.92 (9)
C21-W2-P	124.6 (2)	S1-Fe1-W2	56.04 (6)
C21-W2-Fe2	85.8 (2)	S2-Fe1-W2	56.46 (7)
C21-W2-Fe1	135.8 (2)	C41-Fe2-S1	92.6 (3)
C22-W2-C23	120.0 (4)	C41-Fe2-S2	162.6 (3)
C22-W2-S1	136.7 (3)	C41-Fe2-W2	106.1 (3)
C22-W2-S2	89.3 (2)	C43-Fe2-S1	159.9 (3)
C22-W2-P	74.3 (3)	C43-Fe2-S2	91.9 (3)
C22-W2-Fe2	87.4 (3)	C43-Fe2-W2	103.9 (3)
C22-W2-Fe1	138.2 (2)	C42-Fe2-S1	101.4 (3)
C23-W2-S1	95.0 (2)	C42-Fe2-S2	97.5 (3)
C23-W2-S2	143.1 (3)	C42-Fe2-W2	146.2 (3)
C23-W2-P	77.2 (2)	S1-Fe2-S2	79.65 (8)
C23-W2-Fe2	142.2 (2)	S1-Fe2-W2	56.27 (6)
C23-W2-Fe1	94.8 (3)	S2-Fe2-W2	56.62 (6)
S1-W2-S2	73.08 (7)	Fe1-S1-Fe2	99.1 (1)
S1-W2-P	143.01 (8)	Fe1-S1-W2	73.56 (7)
S1-W2-Fe2	50.65 (6)	Fe1-S1-W1	127.3 (1)
S1-W2-Fe1	50.40 (5)	Fe2-S1-W2	73.08 (7)
S2-W2-P	91.58 (8)	Fe2-S1-W1	127.3 (1)
S2-W2-Fe2	50.92 (6)	W2-S1-W1	137.2 (1)
S2-W2-Fe1	50.46 (6)	Fe1-S2-Fe2	98.39 (9)
P-W2-Fe2	138.91 (6)	Fe1-S2-W2	73.08 (7)
P-W2-Fe1	93.76 (6)	Fe2-S2-W2	72.46 (7)
Fe2-W2-Fe1	75.64 (4)	C57-P-W2	112.8 (3)
C32-Fe1-S1	93.5 (3)	C58-P-W2	116.9 (3)
C32-Fe1-S2	157.3 (3)	C51-P-W2	115.4 (3)
C32-Fe1-W2	101.8 (3)	O-C-M(av)	178 (1)

Structure of 8. An ORTEP drawing of the molecular structure of 8 is shown in Figure 4. Intramolecular bond distances and selected bond angles are listed in Tables IX and X. Compound 8 is similar to 5 since it contains a tungsten carbonyl group attached on one of the triply bridging sulfido ligands of an open $M_3(\mu_3-S)_2$ cluster. The principal differences between 5 and 8 are that the $M_3(\mu_3-S)_2$ grouping in 8 is the compound 6, while in 5, it is 1. Also, the tungsten grouping in 8 is $W(CO)_5$, while in 5, it is $W(CO)_4PMe_2Ph$. There are no significant structural differences between the free molecule of 5 and the unit of 5 in 8 that acts as a ligand to the $W(CO)_5$ group. The W1-S1 distance in 8 is 2.537 (2) Å and is significantly longer than the corresponding bond in 5 but is similar to those in 9¹⁶ and 10.¹⁹

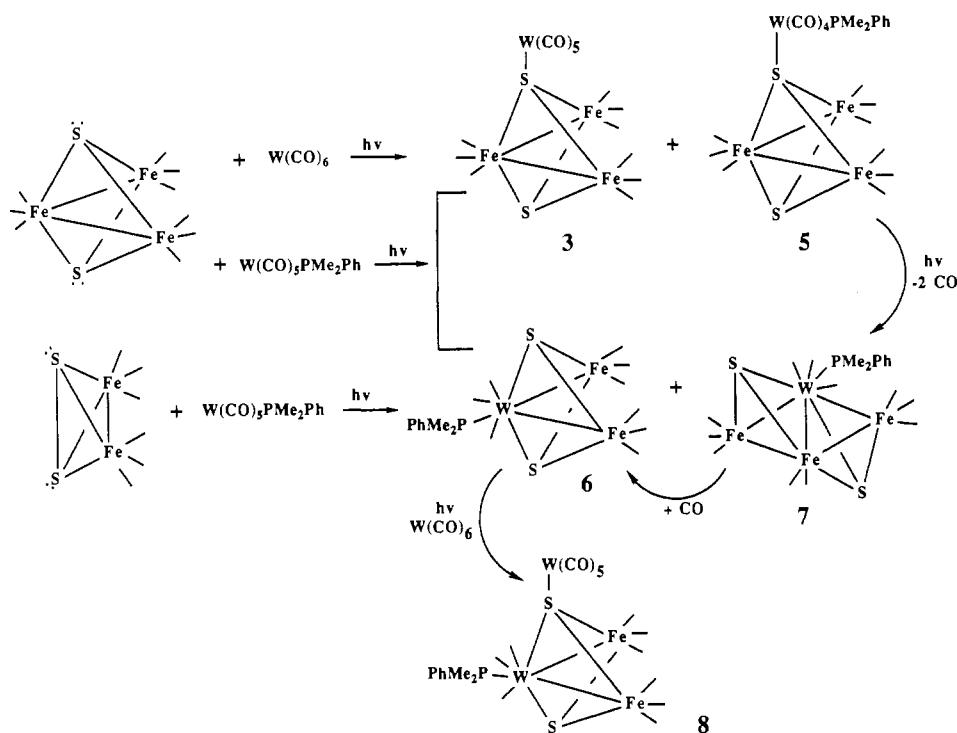
Discussion

The results of this study are summarized in Scheme I. UV irradiation of solutions of 1 and $W(CO)_5$ has yielded compound 3 which is a $W(CO)_5$ adduct of 1. A similar product was obtained

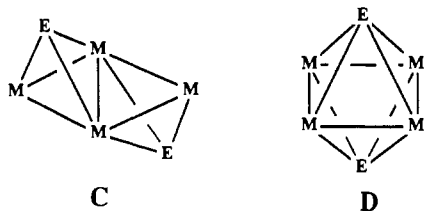
(22) Wakatsuki, Y.; Yamazaki, H.; Cheng, G. *J. Organomet. Chem.* **1988**, *347*, 151.

(23) Cotton, F. A. *Prog. Inorg. Chem.* **1976**, *21*, 1.

Scheme I

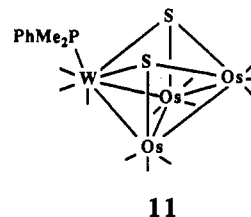


from the reaction of $\text{Os}_3(\text{CO})_9(\mu_3\text{-S})_2$ and $\text{W}(\text{CO})_6$ under UV irradiation.¹¹ The reaction of **1** with $\text{W}(\text{CO})_5\text{PMe}_2\text{Ph}$ under UV irradiation yielded two adducts, **3** and **5**. The former was formed by loss of PMe_2Ph from $\text{W}(\text{CO})_5\text{PMe}_2\text{Ph}$, and the latter was formed by loss of CO. No metal-metal bonds were made in the formation of **3** and **5**. However, in addition to **3** and **5**, the butterfly cluster **7** and the metal-metal-exchange product **6** were also obtained from the reaction of **1** with $\text{W}(\text{CO})_5\text{PMe}_2\text{Ph}$. Compound **7** appears to be derived from **5** since longer reaction periods gave higher yields of **7** and an independent irradiation of **5** gave the highest yield of **7**. The **5** to **7** transformation is believed to occur intramolecularly although this is not proved by these experiments. The conversion of **5** to **7** involves the loss of 2 mol of CO and the transformation of the quadruply bridging sulfido ligand into a triply bridging ligand. The two steps resulted in the loss of six electrons from the metal atoms, and as a result, three metal-metal bonds were formed. Accordingly, compound **7** adopts the electron-precise butterfly tetrahedral structure C. However, there is the alternative structure D that has been found frequently



for 62-electron tetranuclear metal clusters.²⁴ Structure D consists of a square of four metal atoms with quadruply bridging ligands on opposite sides. These clusters obey the bonding principles of the skeletal electron pair theory.²⁵ The reason that **7** adopts the alternative electron-precise structure C in preference to D is not apparent. The reaction of $\text{Os}_3(\text{CO})_9(\mu_3\text{-S})_2$ with $\text{W}(\text{CO})_5$ -

(PMe_2Ph) under UV irradiation yielded the 64-electron cluster $\text{WOs}_3(\text{CO})_{12}(\text{PMe}_2\text{Ph})(\mu_3\text{-S})_2$ (**11**), which possesses a butterfly



cluster in which both sulfido ligands lie on the same side of the cluster.¹² Compound **11** does not give a stable decarbonylation product. In fact, the osmium homologue of **7** has not been prepared.

Compound **6** is the metal-metal-exchange product of **1** and $\text{W}(\text{CO})_5(\text{PMe}_2\text{Ph})$. Although **6** can be obtained in a better yield from the reaction of **2** with $\text{W}(\text{CO})_5(\text{PMe}_2\text{Ph})$, it was also obtained in low yields by the thermal decomposition of **7** under CO. It is possible that **6** may have been formed by the sequence $\mathbf{5} \rightarrow \mathbf{7} \rightarrow \mathbf{6}$, in the original reaction of **1** with $\text{W}(\text{CO})_5(\text{PMe}_2\text{Ph})$, but efforts to obtain **6** by irradiation of samples of **7** under nitrogen were unsuccessful. Since small amounts of **2** were isolated from the reaction of **1** with $\text{W}(\text{CO})_5(\text{PMe}_2\text{Ph})$, it is possible that small amounts of **6** that were obtained could have been formed by a secondary reaction of **2** with $\text{W}(\text{CO})_5(\text{PMe}_2\text{Ph})$.

The transformation of **5** to **7** is significant because it implies that the interaction of the sulfido ligand with the incoming fragment is an important requisite to the formation of **7** from **1** and $\text{W}(\text{CO})_5(\text{PMe}_2\text{Ph})$. In contrast, in the enlargement of the cluster complex $\text{Mo}_2\text{Ru}(\text{CO})_7\text{Cp}_2(\mu_3\text{-S})$ by the addition of mononuclear ruthenium carbonyl fragments, evidence for interaction of the fragments with the oxygen atoms of the CO ligands was obtained.²⁶

The product **8** was formed simply by the addition of a $\text{W}(\text{CO})_5$ group to one of the sulfido ligands of **6**. It was a minor product in the reaction of **2** with $\text{W}(\text{CO})_5(\text{PMe}_2\text{Ph})$ but was obtained in a reasonable yield by the reaction of **6** with $\text{W}(\text{CO})_6$ in the presence of UV irradiation.

In the reactions of **1** and $\text{Os}_3(\text{CO})_9(\mu_3\text{-S})_2$ with $\text{W}(\text{CO})_6$, no products containing tungsten-iron or tungsten-osmium bonds were

(24) (a) Vahrenkamp, H.; Wolters, D. *J. Organomet. Chem.* **1982**, *224*, C17. (b) Field, J. S.; Haines, R. J.; Smit, D. N. *J. Organomet. Chem.* **1982**, *224*, C49.

(25) (a) Mingos, D. M. P. *Acc. Chem. Res.* **1984**, *17*, 311. (b) Mingos, D. M. P.; Johnston, R. L. *Struct. Bonding* **1987**, *68*, 29. (c) Wade, K. In *Transition Metal Clusters*; Johnson, B. F. G., Ed.; John Wiley and Sons: New York, 1980. (d) Johnson, B. F. G.; Benfield, R. E. In *Topics in Stereochemistry*; Geoffroy, G. L., Ed.; John Wiley and Sons: New York, 1981; Vol. 12.

(26) Adams, R. D.; Babin, J. E.; Tasi, M. *Inorg. Chem.* **1988**, *27*, 2618.

obtained. However, in the reactions of **1** and $\text{Os}_3(\text{CO})_9(\mu_3\text{-S})_2$ with $\text{W}(\text{CO})_5(\text{PMe}_2\text{Ph})$, several products **6**, **7**, and **11** containing tungsten–iron and tungsten–osmium bonds were obtained. In all such cases, the tungsten atom contains a PMe_2Ph ligand. It is believed that the removal of electron density from the metal atoms is unfavorable to metal–metal bond formation;²⁷ thus, the substitution of phosphine ligands, which are not as effective in electron density withdrawal as CO ligands, may favor the formation of metal–metal bonds.

Acknowledgment. The research was supported by the National

(27) Cotton, F. A. *Acc. Chem. Res.* 1969, 2, 240.

Science Foundation under Grant No. CHE-8612862. The AM-300 NMR spectrometer was purchased with funds from the National Science Foundation, Grant No. CHE-8411172.

Registry No. 1, 22309-04-2; 2, 14243-23-3; 3, 118514-44-6; 4, 118514-45-7; 5, 118514-46-8; 6, 118514-47-9; 7, 118514-48-0; 8, 118514-49-1; $\text{W}(\text{CO})_6$, 14040-11-0; $\text{W}(\text{CO})_5(\text{PMe}_2\text{Ph})$, 42565-94-6; W, 7440-33-7; Fe, 7439-89-6.

Supplementary Material Available: Tables of crystallographic data, positional parameters and $B(\text{eq})$ values, and anisotropic thermal parameters (U values) for **5–8** (15 pages); tables of structure factor amplitudes for all four structural analyses (79 pages). Ordering information is given on any current masthead page.

Contribution from the Department of Chemistry, Faculty of Science, Kyoto University, Sakyo-ku, Kyoto 606, Japan, Department of Chemistry, Faculty of Science, Ehime University, Matsuyama 790, Japan, and Faculty of Pharmaceutical Sciences, University of Tokushima, Tokushima 770, Japan

Direct Evidence of Heme–*tert*-Butyl Peroxide Adduct Formation Demonstrated by Simultaneous ESR and Optical Measurements

Kunihiko Tajima,^{*,†,‡} Junichi Jinno,[‡] Kazuhiko Ishizu,[‡] Hiromu Sakurai,[§] and Hiroaki Ohya-Nishiguchi[†]

Received February 17, 1988

A possible model of a heme protein–peroxide complex has been obtained by mixing chloro(5,10,15,20-tetraphenylporphyrinato)iron(III) ($\text{Fe}^{\text{III}}(\text{TPP})\text{Cl}$) with *tert*-butyl hydroperoxide (BHPO) in the presence of alkaline reagents. The ESR and optical absorption spectra were simultaneously measured for the frozen solution at 77 K. The observed optical spectra showed Soret, β , and α band absorption maxima at 420, 543, and 571 nm. The ESR spectra show that this iron complex takes the low-spin ferric state with an anomalously small g anisotropy ($g_1 = 1.96$, $g_2 = 2.15$, and $g_3 = 2.30$). It has been shown from thaw-and-freeze ESR measurements that this complex is very unstable above 5 °C and readily decomposes to non-heme iron type species such as open-chain polypyrrole complexes. On the basis of the ESR spectrometric titration carried out by changing the mixing molar ratio of BHPO and NaOCH_3 , the coordination structure of the intermediate complex is concluded to be a six-coordinate $\text{Fe}^{\text{III}}(\text{TPP}(\text{OCH}_3))(\text{OOC}(\text{CH}_3)_3)$ complex. The crystal-field parameters estimated by Bohan's treatment indicate that the peroxide anion causes a strong axial distortion toward the ferric ion, compared with the usual nitrogenous and oxygenous donors. The present complex would be the first example of a low-spin six-coordinate ferric alkyl peroxide complex.

Introduction

Mechanisms of the reactions occurring between peroxides and porphyrin–iron complexes have attracted extensive attention from researchers of heme chemistry, since some classes of heme enzymes showed their enzymatic activities in the presence of peroxides.² For example, (1) in the oxidation process of some organic molecules in the presence of horseradish peroxidase (HRP), the addition of hydrogen peroxide starts the enzymatic action of HRP,³ and (2) alkyl hydroperoxides or acyl peroxides readily activate the monooxygenases such as cytochrome P-450 in the absence of oxygen and reductase.⁴ One oxygen atom of the peroxide moiety in acyl peroxides is inserted into a wide variety of substrate molecules, and (3) the catalases⁵ promote the decomposition of hydrogen peroxide to water and oxygen to inhibit the biological damages caused by hydrogen peroxide. These heme enzymes have distinctively different biological functions, but it has been concluded that the heme chromophores commonly form heme–peroxide adducts as an intermediate in the earlier reaction stage of their enzymatic actions.⁴ Such intermediate peroxide adducts have been regarded as an important species in catalytic reaction cycles of these heme enzymes, since higher valent oxoiron complexes called Compound I² are successively generated from the iron peroxide complexes. Model systems composed of synthetic porphyrin–iron complexes and several oxidants such as alkyl hydroperoxides and acyl peroxides⁶ have extensively been studied to understand the peculiar electronic structure and chemical re-

activity of heme–oxo or heme–peroxo complexes. For example, Groves et al.⁷ reported that the (5,10,15,20-tetrakis(2,4,6-trimethylphenyl)porphyrinato)iron(III) complex reacts with *m*-chloroperbenzoic acid to form an oxoiron(IV) π cation radical species. However, the profile for the coordination structures of iron peroxide complexes has not fully been established in spite of the important relevance to such intermediate species generated in the reaction processes of heme enzymes such as monooxygenase, peroxidase, and catalase.

Recently, we have proposed that an intermediate formed in the reaction system composed of the tetraphenylporphyrin–iron complex ($\text{Fe}^{\text{III}}(\text{TPP})\text{Cl}$) and *tert*-butyl hydroperoxide (BHPO) in the presence of an alkaline reagent such as tetramethylammonium hydroxide ((TMA)OH) can be regarded as a possible model complex⁸ of these heme–peroxide intermediates.⁹ The ESR

- (1) On leave from the Department of Chemistry, Faculty of Science, Ehime University, Matsuyama 790, Japan.
- (2) Dunford, H. B.; Stillmann, J. S. *Coord. Chem. Rev.* 1976, 19, 187.
- (3) Dolphin, D.; Felton, R. H. *Acc. Chem. Res.* 1974, 7, 26.
- (4) (a) White, R. E.; Coon, M. *J. Annu. Rev. Biochem.* 1980, 49, 315. (b) Groves, J. T.; Krishnan, S.; Avaria, G. E.; Nemo, T. E. In *Biomimetic Chemistry*; Dolphin, D., McKenna, C., Murakami, Y., Tabushi, I., Eds.; Advances in Chemistry 191; American Chemical Society: Washington, DC, 1980; p 277.
- (5) Schonbaum, G. R.; Chance, B. In *The Enzymes*, 3rd ed.; Boyer, P. D., Ed.; Academic Press: New York, 1973; Vol. 8C, p 363.
- (6) (a) Groves, J. T.; Watanabe, Y. *J. Am. Chem. Soc.* 1986, 108, 7834. (b) Groves, J. T.; Watanabe, Y. *Inorg. Chem.* 1987, 26, 785.
- (7) (a) Groves, J. T.; Haushalter, R. C.; Nakamura, M.; Nemo, T. E.; Evans, B. J. *J. Am. Chem. Soc.* 1981, 103, 2884. (b) Groves, J. T.; Nemo, T. E. *J. Am. Chem. Soc.* 1983, 105, 5786.
- (8) Tajima, K.; Ishizu, K.; Sakurai, H.; Ohya-Nishiguchi, H. *Biochem. Biophys. Res. Commun.* 1986, 135, 972.

[†] Kyoto University.

[‡] Ehime University.

[§] University of Tokushima.